LEIBNIZ-INFORMATIONSZENTRUM
TECHNIK UND NATURWISSENSCHAFTEN
UNIVERSITÄTSBIBLIOTHEK

TIB

FAIR scientific information with the Open Research Knowledge Graph

Markus Stocker
November 14, 2022
EOSC Symposium

Leibniz Gemeinschaft

failure than in LV tissue samples from unused donor hearts (*Figure 1A*). As shown by electrophoretic mobility shift assays, IRE binding activity was significantly reduced in failing hearts (most pronounced in patients with ischemic cardiomyopathy) (*Figure 1B*). Protein expression levels of the transferrin receptor were significantly lower in failing hearts than in the controls (*Figure 1C*).

Targeted Irp deletion in mice induces ID in the myocardium

We generated mice with a cardiomyocyte-targeted deletion of *Irp1* and *Irp2* (Cre-Irp1/2^{0f}) to address Irp function in the heart (*Figure 2A*). Cre-Irp1/2^{0f} mice were born at the expected Mendelian inheritance ratio and survived into adulthood. Reverse transcriptase polymerase chain reaction on LV myocardium and isolated cardiomyocytes demonstrated near-complete Cre-mediated deletion of Irp1 and Irp2 mRNAs in cardiomyocytes from Cre-Irp1/2$^{f/f}$ mice compared with littermates lacking the Cre transgene (Irp1/2^{0f}) (*Figure 2B*). Irp1 and Irp2 protein expression was markedly reduced in LV myocardium and barely detectable in isolated cardiomyocytes from Cre-Irp1/2^{0f} mice (*Figure 2C and D*). Irp1 and Irp2 protein expression in the liver was similar in Cre-Irp1/2$^{f/f}$ and Irp1/2$^{f/f}$ mice (*Figure 2C* and *D*). IRE binding activity was strongly reduced in isolated cardiomyocytes from Cre-Irp1/2^{0f} mice (*Figure 2E*), confirming near-complete Cre-mediated recombination. Iron-regulatory protein/IRE-regulated proteins involved in iron transport and storage were differentially regulated in cardiomyocytes from Cre-Irp1/2^{0f} mice: the transferrin receptor was down-regulated (25 ± 14% of Irp1/2$^{f/f}$ controls, $P = 0.006$), whereas ferroportin (325 ± 9%, $P = 0.003$) and ferritin H-chain (249 ± 35%, $P = 0.012$) were up-regulated ($n = 3$ per group; representative immunoblots are presented in *Figure 2F*). As a result, iron concentration in cardiomyocytes was significantly reduced in Cre-Irp1/2^{0f} mice (*Figure 2G*). Likewise, iron concentration in the left ventricle was reduced in Cre-Irp1/2^{0f} mice compared with Irp1/2^{0f} controls, whereas iron concentrations in the M. quadriceps femoris and liver were not affected (*Figure 2H*). Iron concentration in the left ventricle was normal in Cre mice showing that cardiac ID in Cre-Irp1/2^{0f} mice was not related to Cre transgene expression per se (*Figure 2H*). Haem and myoglobin concentrations were significantly reduced in the left ventricle of Cre-Irp1/2^{0f} mice (*Figure 2I* and *J*). Copper and free radical concentrations in the left ventricle were similar in Cre-Irp1/2$^{f/f}$ and Irp1/2^{0f} mice (see Supplementary material online, *Figure S2*).

Cre-Irp1/2^{0f} mice did not show an obvious phenotype under baseline conditions. Body mass, heart mass, LV mass, and cardiomyocyte cross-sectional area were similar in Cre-Irp1/2^{0f} and Irp1/2^{0f} mice under baseline conditions (see Supplementary material online, *Table S1*). On echocardiography, LV end-diastolic and end-systolic dimensions and LV systolic and diastolic function were similar in both genotypes (see Supplementary material online, *Table S1*). Cre-Irp1/2^{0f} mice were not anaemic and had a normal peripheral blood count (see Supplementary material online, *Table S2*).

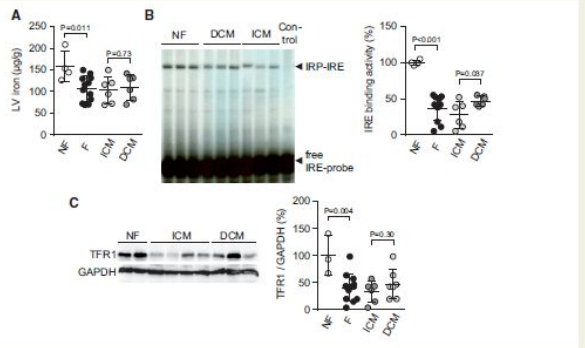

Figure 1 *Reduced IRP activity and iron content in failing human hearts.* (A) Non-haem iron concentration in left ventricular (LV) tissue samples from non-failing donors (NF) and patients with cardiac failure (*F*) due to ischemic cardiomyopathy (ICM) or dilated cardiomyopathy (DCM); $n = 4$–6 per group. (B) Representative electrophoretic mobility shift assay and summary data showing iron-responsive element (IRE) binding activity in LV tissue samples; $n = 4$–6 (control, no sample loaded). (C) Representative immunoblot and summary data showing transferrin receptor 1 (TFR1) and GAPDH protein expression in LV tissue samples; $n = 3$–7. *P* values were determined by two independent sample *t*-test.

https://doi.org/10.1093/eurheartj/ehw333

Scientific information is data
This data is not FAIR
Certainly not for machines

We find and access documents

failure than in LV tissue samples from unused donor hearts (*Figure 1A*). As shown by electrophoretic mobility shift assays, IRE binding activity was significantly reduced in failing hearts (most pronounced in patients with ischemic cardiomyopathy) (*Figure 1B*). Protein expression levels of the transferrin receptor were significantly lower in failing hearts than in the controls (*Figure 1C*).

Targeted Irp deletion in mice induces ID in the myocardium

We generated mice with a cardiomyocyte-targeted deletion of *Irp1* and *Irp2* (Cre-Irp1/2$^{0/f}$) to address Irp function in the heart (*Figure 2A*). Cre-Irp1/2$^{0/f}$ mice were born at the expected Mendelian inheritance ratio and survived into adulthood. Reverse transcriptase polymerase chain reaction on LV myocardium and isolated cardiomyocytes demonstrated near-complete Cre-mediated deletion of Irp1 and Irp2 mRNAs in cardiomyocytes from Cre-Irp1/2$^{f/f}$ mice compared with littermates lacking the Cre transgene (Irp1/2$^{f/f}$) (*Figure 2B*). Irp1 and Irp2 protein expression was markedly reduced in LV myocardium and barely detectable in isolated cardiomyocytes from Cre-Irp1/2$^{0/f}$ mice (*Figure 2C and D*). Irp1 and Irp2 protein expression in the liver was similar in Cre-Irp1/2$^{f/f}$ and Irp1/2$^{f/f}$ mice (*Figure 2C* and D). IRE binding activity was strongly reduced in isolated cardiomyocytes from Cre-Irp1/2$^{0/f}$ mice (*Figure 2E*), confirming near-complete Cre-mediated recombination. Iron-regulatory protein/IRE-regulated proteins involved in iron transport and storage were differentially

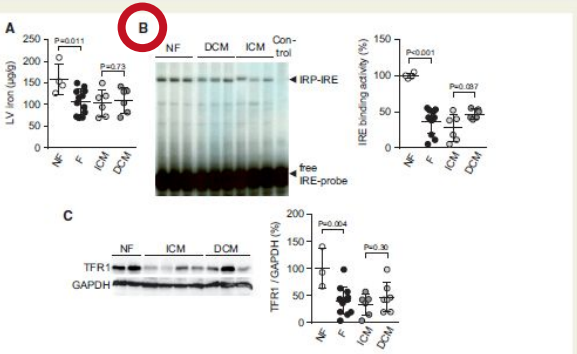

Figure 1 *Reduced IRP activity and iron content in failing human hearts.* (A) Non-haem iron concentration in left ventricular (LV) tissue samples from non-failing donors (NF) and patients with cardiac failure (F) due to ischemic cardiomyopathy (ICM) or dilated cardiomyopathy (DCM); $n = 4$–6 per group. (B) Representative electrophoretic mobility shift assay and summary data showing iron-responsive element (IRE) binding activity in LV tissue samples; $n = 4$–6 (control, no sample loaded). (C) Representative immunoblot and summary data showing transferrin receptor 1 (TFR1) and GAPDH protein expression in LV tissue samples; $n = 3$–7. *P* values were determined by two independent sample *t*-test.

https://doi.org/10.1093/eurheartj/ehw333

failure than in LV tissue samples from unused donor hearts (*Figure 1A*). As shown by electrophoretic mobility shift assays, IRE binding activity was significantly reduced in failing hearts (most pronounced in patients with ischemic cardiomyopathy) (*Figure 1B*). Protein expression levels of the transferrin receptor were significantly lower in failing hearts than in the controls (*Figure 1C*).

failure than in LV tissue samples from unused donor hearts (*Figure 1A*). As shown by electrophoretic mobility shift assays, IRE binding activity was significantly reduced in failing hearts (most pronounced in patients with ischemic cardiomyopathy) (*Figure 1B*). Protein expression levels of the transferrin receptor were significantly lower in failing hearts than in the controls (*Figure 1C*).

Targeted Irp deletion in mice induces ID in the myocardium

We generated mice with a cardiomyocyte-targeted deletion of *Irp1* and *Irp2* (Cre-Irp1/2$^{0/}$) to address Irp function in the heart (*Figure 2A*). Cre-Irp1/2$^{0/}$ mice were born at the expected Mendelian inheritance ratio and survived into adulthood. Reverse transcriptase polymerase chain reaction on LV myocardium and isolated cardiomyocytes demonstrated near-complete Cre-mediated deletion of Irp1 and Irp2 mRNAs in cardiomyocytes from Cre-Irp1/2$^{f/f}$ mice compared with littermates lacking the Cre transgene (Irp1/2$^{f/f}$) (*Figure 2B*). Irp1 and Irp2 protein expression was markedly reduced in LV myocardium and barely detectable in isolated cardiomyocytes from Cre-Irp1/2$^{0/}$ mice (*Figure 2C and D*). Irp1 and Irp2 protein expression in the liver was similar in Cre-Irp1/2$^{f/f}$ and Irp1/2$^{f/f}$ mice (*Figure 2C and D*). IRE binding activity was strongly reduced in isolated cardiomyocytes from Cre-Irp1/2$^{0/}$ mice (*Figure 2E*), confirming near-complete Cre-mediated recombination. Iron-regulatory protein/IRE-regulated proteins involved in iron transport and storage were differentially regulated in card

per group; represent
2F). As a result, iron con
cantly reduced in Cre-I
concentration in the lef
mice compared with Irp
tions in the M. quadrice
(*Figure 2H*). Iron concent
Cre mice showing that
related to Cre transgen
and myoglobin concentr
left ventricle of Cre-Irp1/2
free radical concentrations in the left ventricle were similar in Cre-Irp1/2$^{f/f}$ and Irp1/2$^{0/}$ mice (see Supplementary material online, *Figure S2*).

Cre-Irp1/2$^{0/}$ mice did not show an obvious phenotype under baseline conditions. Body mass, heart mass, LV mass, and cardiomyocyte cross-sectional area were similar in Cre-Irp1/2$^{0/}$ and Irp1/2$^{0/}$ mice under baseline conditions (see Supplementary material online, *Table S1*). On echocardiography, LV end-diastolic and end-systolic dimensions and LV systolic and diastolic function were similar in both genotypes (see Supplementary material online, *Table S1*). Cre-Irp1/2$^{0/}$ mice were not anaemic and had a normal peripheral blood count (see Supplementary material online, *Table S2*).

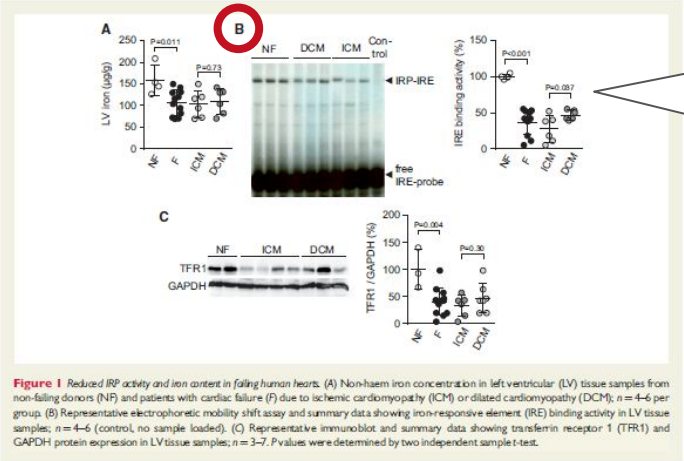

Figure 1 *Reduced IRP activity and iron content in failing human hearts.* (A) Non-haem iron concentration in left ventricular (LV) tissue samples from non-failing donors (NF) and patients with cardiac failure (*F*) due to ischemic cardiomyopathy (ICM) or dilated cardiomyopathy (DCM); $n = 4$–6 per group. (B) Representative electrophoretic mobility shift assay and summary data showing iron-responsive element (IRE) binding activity in LV tissue samples; $n = 4$–6 (control, no sample loaded). (C) Representative immunoblot and summary data showing transferrin receptor 1 (TFR1) and GAPDH protein expression in LV tissue samples; $n = 3$–7. *P* values were determined by two independent sample *t*-test.

CSV

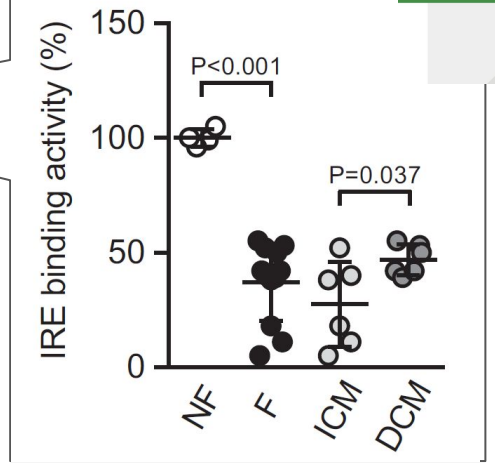

https://doi.org/10.1093/eurheartj/ehw333

failure than in LV tissue samples from unused donor hearts (*Figure 1A*). As shown by electrophoretic mobility shift assays, IRE binding activity was significantly reduced in failing hearts (most pronounced in patients with ischemic cardiomyopathy) (*Figure 1B*). Protein expression levels of the transferrin receptor were significantly lower in failing hearts than in the controls (*Figure 1C*).

Targeted Irp deletion in mice induces ID in the myocardium

We generated mice with a cardiomyocyte-targeted deletion of *Irp1* and *Irp2* (Cre-Irp1/2$^{0/f}$) to address Irp function in the heart (*Figure 2A*). Cre-Irp1/2$^{0/f}$ mice were born at the expected Mendelian inheritance ratio and survived into adulthood. Reverse transcriptase polymerase chain reaction on LV myocardium and isolated cardiomyocytes demonstrated near-complete Cre-mediated deletion of Irp1 and Irp2 mRNAs in cardiomyocytes from Cre-Irp1/2$^{f/f}$ mice compared with littermates lacking the Cre transgene (Irp1/2$^{0/f}$) (*Figure 2B*). Irp1 and Irp2 protein expression was markedly reduced in LV myocardium and barely detectable in isolated cardiomyocytes from Cre-Irp1/2$^{0/f}$ mice (*Figure 2C and D*). Irp1 and Irp2 protein expression in the liver was similar in Cre-Irp1/2$^{f/f}$ and Irp1/2$^{f/f}$ mice (*Figure 2C* and D). IRE binding activity was strongly reduced in isolated cardiomyocytes from Cre-Irp1/2$^{0/f}$ mice (*Figure 2E*), confirming near-complete Cre-mediated recombination. Iron-regulatory protein/IRE-regulated proteins involved in iron transport and storage were differentially

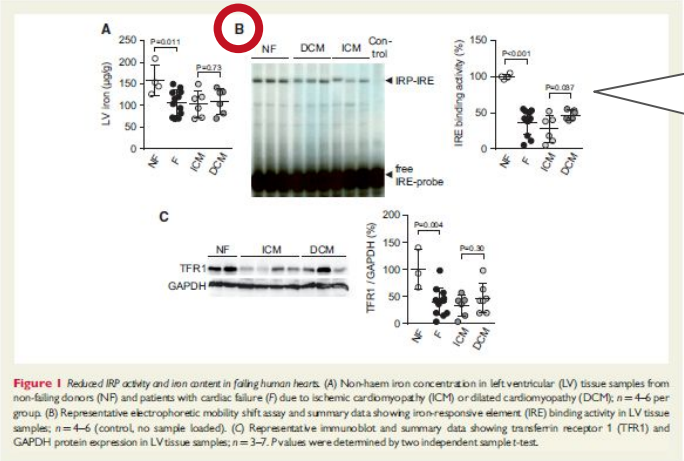

Figure 1 *Reduced IRP activity and iron content in failing human hearts.* (A) Non-haem iron concentration in left ventricular (LV) tissue samples from non-failing donors (NF) and patients with cardiac failure (*F*) due to ischemic cardiomyopathy (ICM) or dilated cardiomyopathy (DCM); $n = 4$–6 per group. (B) Representative electrophoretic mobility shift assay and summary data showing iron-responsive element (IRE) binding activity in LV tissue samples; $n = 4$–6 (control, no sample loaded). (C) Representative immunoblot and summary data showing transferrin receptor 1 (TFR1) and GAPDH protein expression in LV tissue samples; $n = 3$–7. *P* values were determined by two independent sample *t*-test.

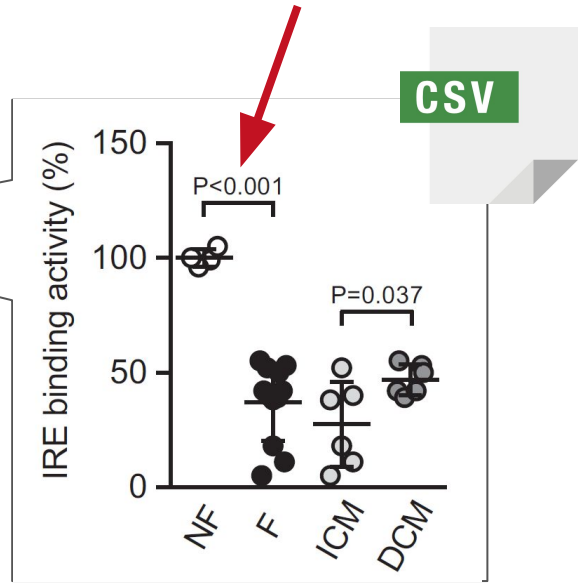

https://doi.org/10.1093/eurheartj/ehw333

This is what machines should consume

Student's t-test [http://purl.obolibrary.org/obo/OBI_0000739]

has dependent variable
iron-responsive element binding [http://amigo.geneontology.org/amigo/term/GO:0030350]

has specified input
CSV
https://doi.org/10.4563/zenodo.56980

has specified output
p-value [http://purl.obolibrary.org/obo/OBI_0000175]
scalar value specification "0.00000000131112475"^^xsd:decimal

https://doi.org/10.1093/eurheartj/ehw333

“Scientific writing can [...] be called *information burying*”

First we bury it and then we mine it again

-- Barend Mons (2005)

https://doi.org/10.1186/1471-2105-6-142

“we have failed to [...] organize [...] information [...] in rigorous [...] ways, so that finding what we want and understanding what's already known become [...] increasingly costly experiences”

-- Teresa K. Attwood et al. (2009)

https://doi.org/10.1042/BJ20091474

“Despite recent developments in machine learning [...], data extraction is still largely a manual process”

-- Julian Higgins et al. (2022)

https://training.cochrane.org/handbook/current

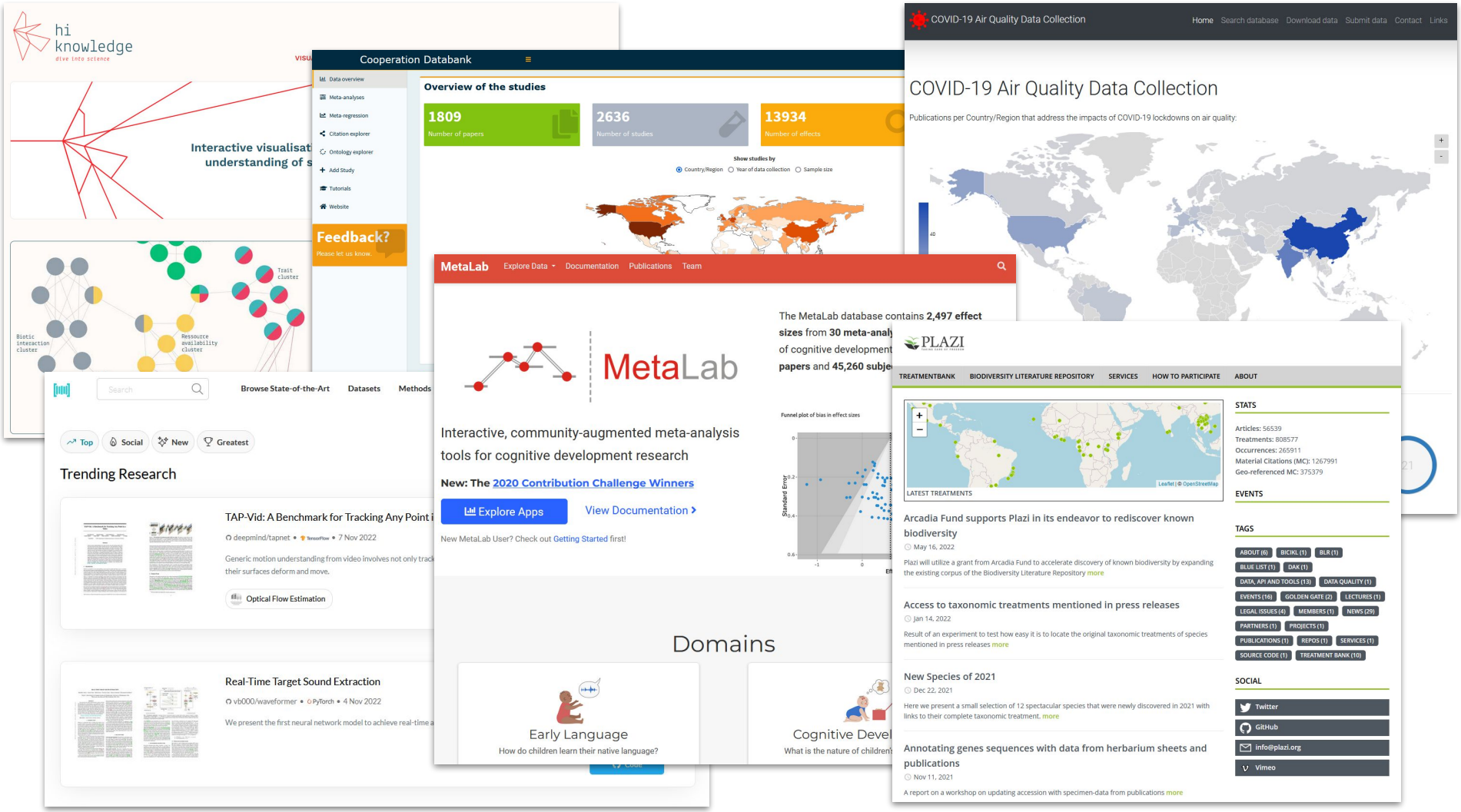
hi knowledge
dive into science
Interactive visualisat
understanding of s
Trait cluster
Biotic interaction cluster
Ressource availability cluster
Cooperation Databank
Data overview
Meta-analyses
Meta-regression
Citation explorer
Ontology explorer
Add Study
Tutorials
Website
Feedback?
Please let us know.
Overview of the studies
1809
Number of papers
2636
Number of studies
13934
Number of effects
Show studies by
Country/Region
Year of data collection
Sample size
COVID-19 Air Quality Data Collection
Home
Search database
Download data
Submit data
Contact
Links
COVID-19 Air Quality Data Collection
Publications per Country/Region that address the impacts of COVID-19 lockdowns on air quality:
MetaLab
Explore Data
Documentation
Publications
Team
MetaLab
Interactive, community-augmented meta-analysis tools for cognitive development research
New: The 2020 Contribution Challenge Winners
Explore Apps
View Documentation
New MetaLab User? Check out Getting Started first!
The MetaLab database contains 2,497 effect sizes from 30 meta-analy
of cognitive development
papers and 45,260 subje
Funnel plot of bias in effect sizes
Standard Error
Search
Browse State-of-the-Art
Datasets
Methods
Top
Social
New
Greatest
Trending Research
TAP-Vid: A Benchmark for Tracking Any Point i
deepmind/tapnet • TensorFlow • 7 Nov 2022
Generic motion understanding from video involves not only track
their surfaces deform and move.
Optical Flow Estimation
Real-Time Target Sound Extraction
vb000/waveformer • PyTorch • 4 Nov 2022
We present the first neural network model to achieve real-time a
Domains
Early Language
How do children learn their native language?
Cognitive Devel
What is the nature of children's
PLAZI
TREATMENTBANK
BIODIVERSITY LITERATURE REPOSITORY
SERVICES
HOW TO PARTICIPATE
ABOUT
LATEST TREATMENTS
Leaflet | © OpenStreetMap
STATS
Articles: 56539
Treatments: 808577
Occurrences: 265911
Material Citations (MC): 1267991
Geo-referenced MC: 375379
EVENTS
TAGS
ABOUT (6)
BICIKL (1)
BLR (1)
BLUE LIST (1)
DAK (1)
DATA, API AND TOOLS (13)
DATA QUALITY (1)
EVENTS (16)
GOLDEN GATE (2)
LECTURES (1)
LEGAL ISSUES (4)
MEMBERS (1)
NEWS (29)
PARTNERS (1)
PROJECTS (1)
PUBLICATIONS (1)
REPOS (1)
SERVICES (1)
SOURCE CODE (1)
TREATMENT BANK (10)
SOCIAL
Twitter
GitHub
info@plazi.org
Vimeo
Arcadia Fund supports Plazi in its endeavor to rediscover known biodiversity
May 16, 2022
Plazi will utilize a grant from Arcadia Fund to accelerate discovery of known biodiversity by expanding the existing corpus of the Biodiversity Literature Repository more
Access to taxonomic treatments mentioned in press releases
Jan 14, 2022
Result of an experiment to test how easy it is to locate the original taxonomic treatments of species mentioned in press releases more
New Species of 2021
Dec 22, 2021
Here we present a small selection of 12 spectacular species that were newly discovered in 2021 with links to their complete taxonomic treatment. more
Annotating genes sequences with data from herbarium sheets and publications
Nov 11, 2021
A report on a workshop on updating accession with specimen-data from publications more

hi knowledge
dive into science

VISUALISATION TOOLS | INFO & VISION | FUNDING | LINKS & PUBLICATIONS | CONTACT

Interactive visualisation tools for a better understanding of science and nature

Invasion biology:
large hypothesis network

Interactive network showing clusters of 39 invasion hypotheses, based on Enders et al. (2020) and the book Invasion Biology: Hypotheses and Evidence (Jeschke & Heger, eds, 2018; CABI, Wallingford, UK). This tool is an extension of the smaller network with 12 hypotheses.

Launch visualisation

PLAZI

TREATMENTBANK | BIODIVERSITY LITERATURE REPOSITORY | SERVICES | HOW TO PARTICIPATE | ABOUT

Arcadia Fund supports Plazi in its endeavor to rediscover known biodiversity
May 16, 2022

Plazi will utilize a grant from Arcadia Fund to accelerate discovery of known biodiversity by expanding the existing corpus of the Biodiversity Literature Repository more

Access to taxonomic treatments mentioned in press releases
Jan 14, 2022

Result of an experiment to test how easy it is to locate the original taxonomic treatments of species mentioned in press releases more

New Species of 2021
Dec 22, 2021

Here we present a small selection of 12 spectacular species that were newly discovered in 2021 with links to their complete taxonomic treatment. more

Annotating genes sequences with data from herbarium sheets and publications
Nov 11, 2021

A report on a workshop on updating accession with specimen-data from publications more

STATS
Articles: 56539
Treatments: 808577
Occurrences: 265911
Material Citations (MC): 1267991
Geo-referenced MC: 375379

EVENTS

TAGS
ABOUT (6) | BICIKL (1) | BLR (1) | BLUE LIST (1) | DAK (1) | DATA, API AND TOOLS (13) | DATA QUALITY (1) | EVENTS (16) | GOLDEN GATE (2) | LECTURES (1) | LEGAL ISSUES (4) | MEMBERS (1) | NEWS (29) | PARTNERS (1) | PROJECTS (1) | PUBLICATIONS (1) | REPOS (1) | SERVICES (1) | SOURCE CODE (1) | TREATMENT BANK (10)

SOCIAL
Twitter
GitHub
info@plazi.org
Vimeo

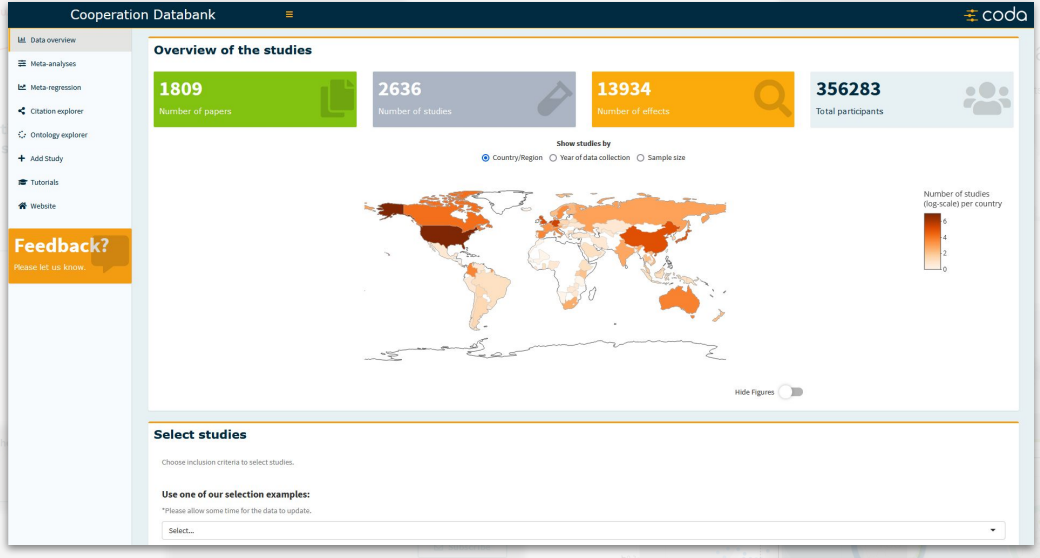
Cooperation Databank
coda
Data overview
Meta-analyses
Meta-regression
Citation explorer
Ontology explorer
Add Study
Tutorials
Website
Feedback?
Please let us know.
Overview of the studies
1809
Number of papers
2636
Number of studies
13934
Number of effects
356283
Total participants
Show studies by
Country/Region
Year of data collection
Sample size
Number of studies (log-scale) per country
Hide Figures
Select studies
Choose inclusion criteria to select studies.
Use one of our selection examples:
*Please allow some time for the data to update.
Select...

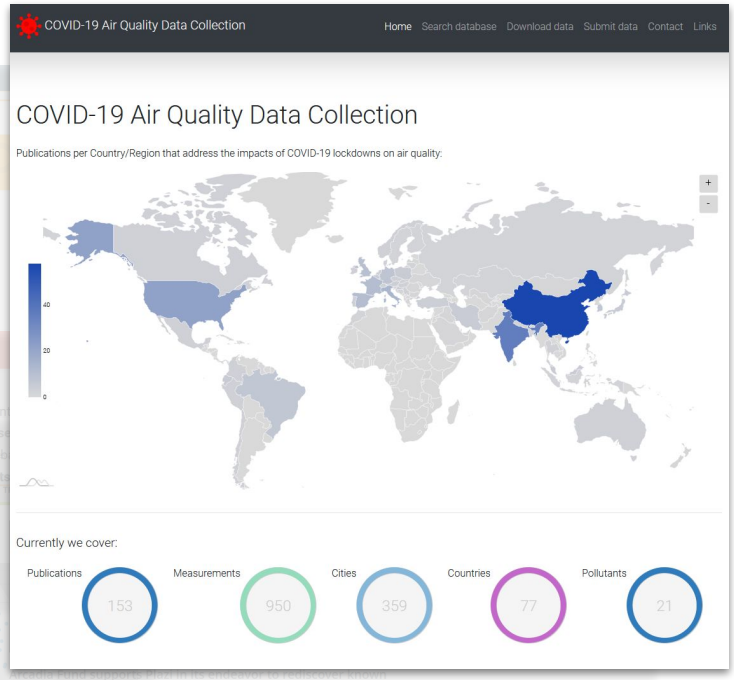
COVID-19 Air Quality Data Collection
Home
Search database
Download data
Submit data
Contact
Links
COVID-19 Air Quality Data Collection
Publications per Country/Region that address the impacts of COVID-19 lockdowns on air quality:
Currently we cover:
Publications
153
Measurements
950
Cities
359
Countries
77
Pollutants
21

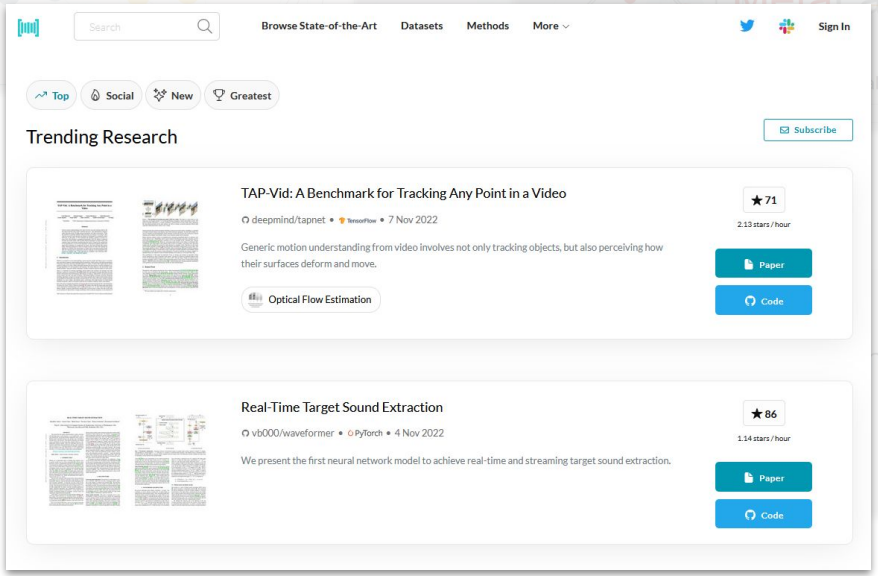
Search
Browse State-of-the-Art
Datasets
Methods
More
Sign In
Top
Social
New
Greatest
Trending Research
Subscribe
TAP-Vid: A Benchmark for Tracking Any Point in a Video
deepmind/tapnet • TensorFlow • 7 Nov 2022
Generic motion understanding from video involves not only tracking objects, but also perceiving how their surfaces deform and move.
Optical Flow Estimation
★ 71
2.13 stars / hour
Paper
Code
Real-Time Target Sound Extraction
vb000/waveformer • PyTorch • 4 Nov 2022
We present the first neural network model to achieve real-time and streaming target sound extraction.
★ 86
1.14 stars / hour
Paper
Code

MetaLab

Interactive, community-augmented meta-analysis tools for cognitive development research

New: The 2020 Contribution Challenge Winners

Explore Apps View Documentation ›

New MetaLab User? Check out Getting Started first!

The MetaLab database contains **2,497 effect sizes** from **30 meta-analyses** across two domains of cognitive development, based on data from **688 papers** and **45,260 subjects**.

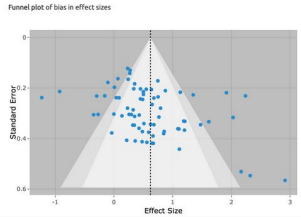

Domains

Early Language

How do children learn their native language?

Cognitive Development

What is the nature of children's understanding?

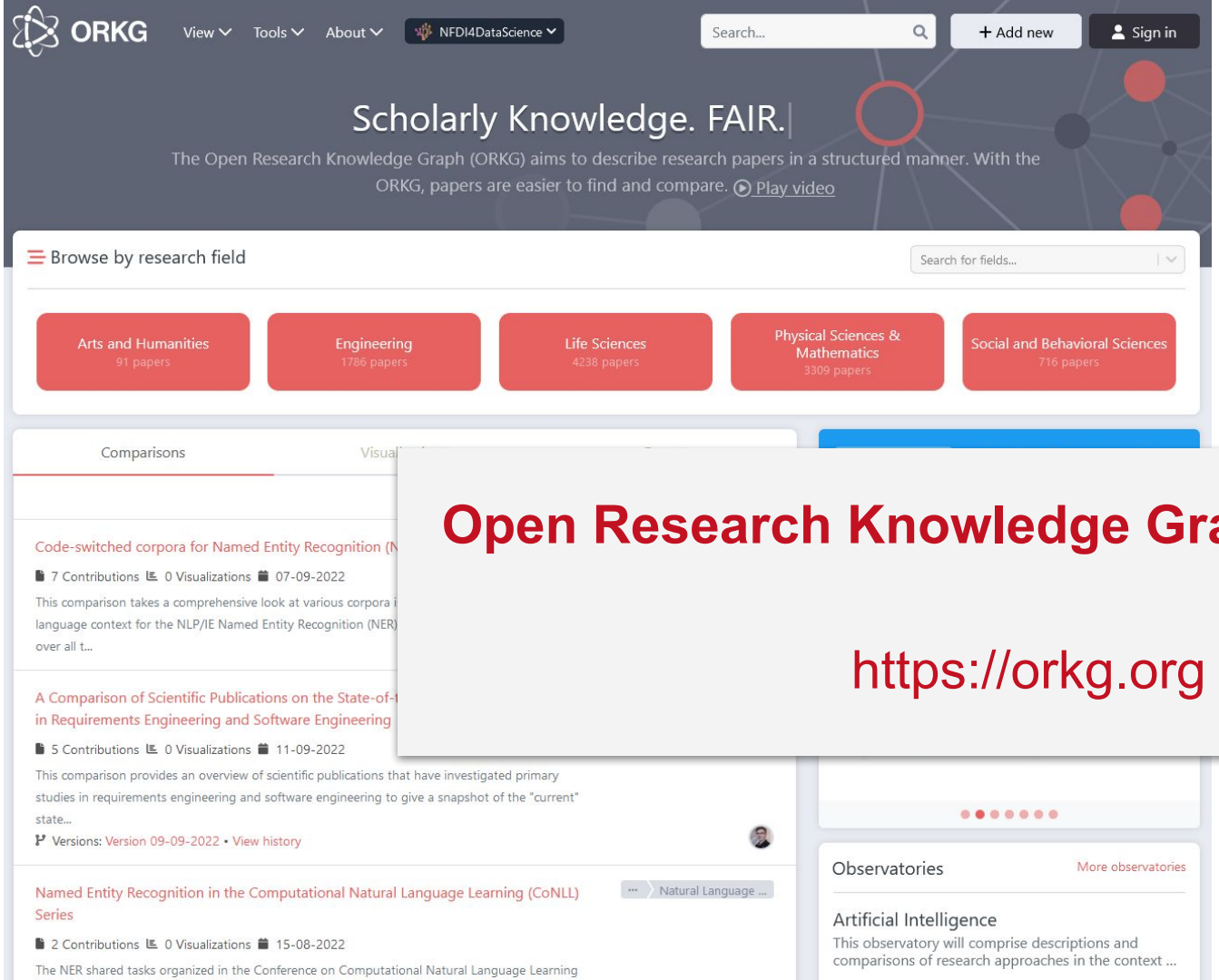

Open Research Knowledge Graph

https://orkg.org • @orkg_org

The benefits are obvious

Properties	Early phase of the COVID-19 outbreak in Lombardy, Italy	Transmission potential of COVID-19 in Iran *2020 - Contribution 1*	Transmission potential of COVID-19 in Iran *2020 - Contribution 2*	Estimating the generation interval for COVID-19 based on symptom onset data *2020 - Contribution 1*
extremely deadly				
deadly				
location	Lombardy, Italy	Iran	Iran	Singapore
has end	2020-03-08	2020-02-29	2020-02-29	2020-02-26
Basic reproduction number	Basic reproduction number estimate value specification	Basic reproduction number estimate value specification	Basic reproduction number estimate value specification	Basic reproduction number estimate value specification
Has value	3.1	3.6	3.58	1.27
not too deadly				
Confidence interval (95%)	Confidence interval (95%)	Confidence interval (95%)	Confidence interval (95%)	Confidence interval (95%)
Lower confidence limit	2.9	3.4	1.29	1.19
Upper confidence limit	3.2	4.2	8.46	1.36

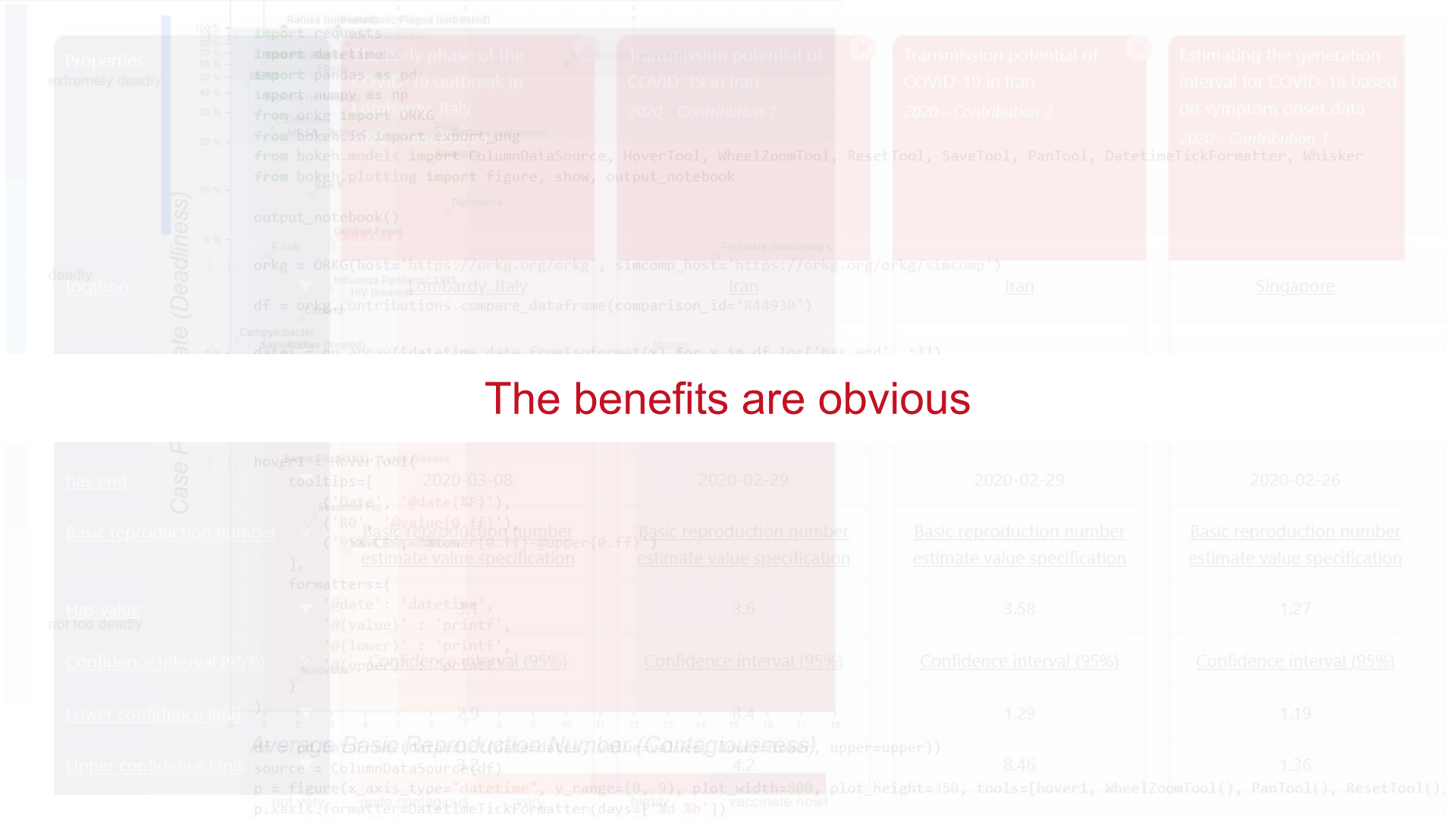

Properties	The early phase of the COVID-19 outbreak in Lombardy, Italy *2020 - Contribution 1*	Transmission potential of COVID-19 in Iran *2020 - Contribution 1*	Transmission potential of COVID-19 in Iran *2020 - Contribution 2*	Estimating the generation interval for COVID-19 based on symptom onset data *2020 - Contribution 1*
location	Lombardy, Italy	Iran	Iran	Singapore
Time period	Time interval	Time interval	Time interval	Time interval
has beginning	2020-01-14	2020-02-19	2020-02-19	2020-01-21
has end	2020-03-08	2020-02-29	2020-02-29	2020-02-26
Basic reproduction number	Basic reproduction number estimate value specification	Basic reproduction number estimate value specification	Basic reproduction number estimate value specification	Basic reproduction number estimate value specification
Has value	3.1	3.6	3.58	1.27
Confidence interval (95%)	Confidence interval (95%)	Confidence interval (95%)	Confidence interval (95%)	Confidence interval (95%)
Lower confidence limit	2.9	3.4	1.29	1.19
Upper confidence limit	3.2	4.2	8.46	1.36

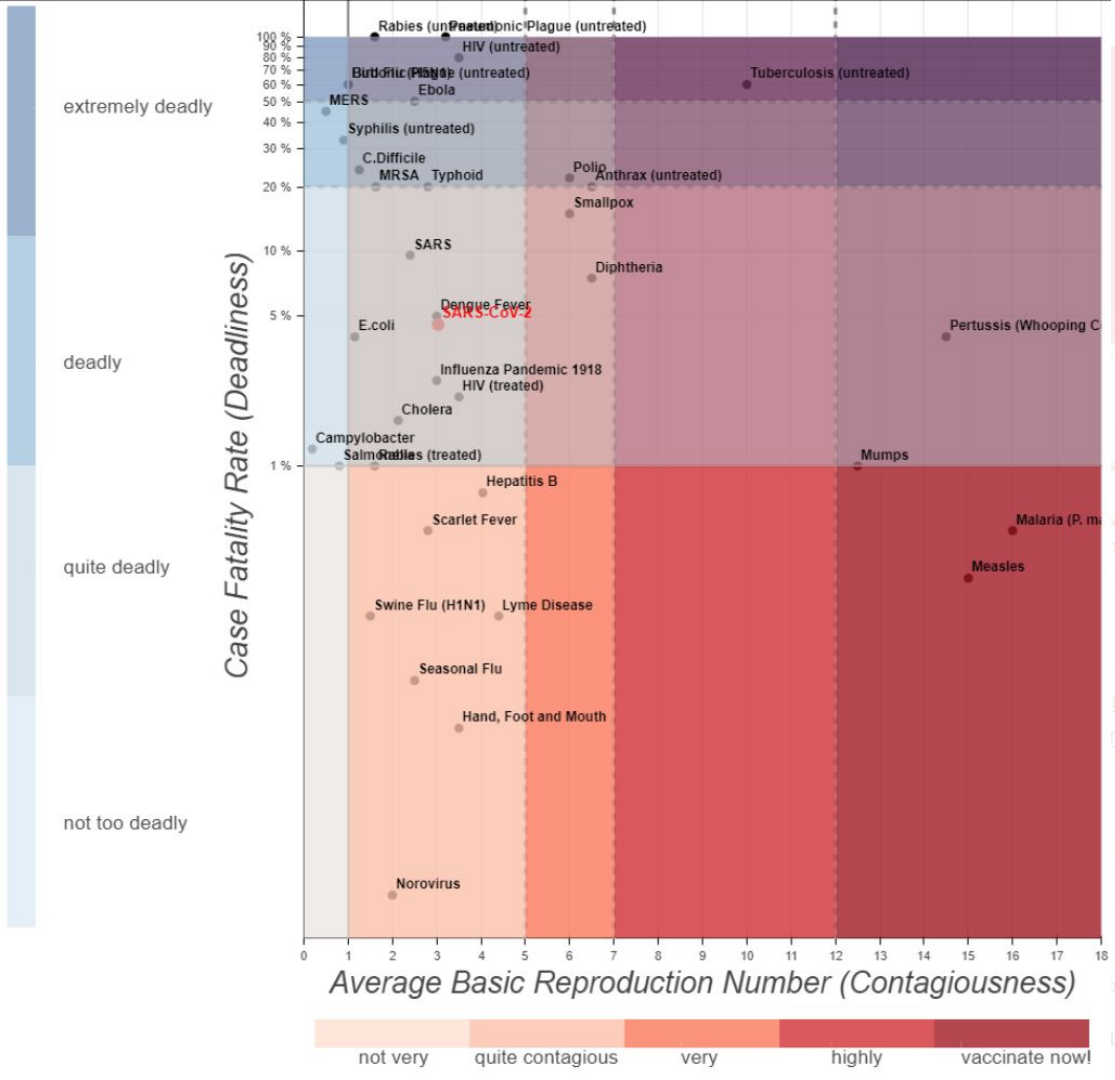

Transmission potential of COVID-19 in Iran

2020 - Contribution 2

Estimating the generation interval for COVID-19 based on symptom onset data

2020 - Contribution 1

ResetTool, SaveTool, PanTool, DatetimeTickFormatter, Whisker

.org/orkg/simcomp')

Iran	Singapore
Time interval	Time interval
2020-02-19	2020-01-21
2020-02-29	2020-02-26
Basic reproduction number estimate value specification	Basic reproduction number estimate value specification
3.58	1.27
Confidence interval (95%)	Confidence interval (95%)
1.29	1.19
8.46	1.36

s end', :]])

er confidence limit', :]])

er confidence limit', :]])

pper=upper))

lot_height=350, tools=[hover1, WheelZoomTool(), PanTool(), ResetTool(),

[ ]:
```
import requests
import datetime
import pandas as pd
import numpy as np
from orkg import ORKG
from bokeh.io import export_png
from bokeh.models import ColumnDataSource, HoverTool, WheelZoomTool, ResetTool, SaveTool, PanTool, DatetimeTickFormatter, Whisker
from bokeh.plotting import figure, show, output_notebook

output_notebook()
```

[ ]:
```
orkg = ORKG(host='https://orkg.org/orkg', simcomp_host='https://orkg.org/orkg/simcomp')

df = orkg.contributions.compare_dataframe(comparison_id='R44930')
```

[ ]:
```
dates = np.array([datetime.date.fromisoformat(x) for x in df.loc['has end', :]])
values = np.float32(df.loc['Has value', :])
lower = np.array([np.float32(x) if x else np.nan for x in df.loc['Lower confidence limit', :]])
upper = np.array([np.float32(x) if x else np.nan for x in df.loc['Upper confidence limit', :]])
```

[ ]:
```
hover1 = HoverTool(
    tooltips=[
        ('Date', '@date{%F}'),
        ('R0', '@value{0.ff}'),
        ('95% CI', '@lower{0.ff}-@upper{0.ff}')
    ],
    formatters={
        '@date': 'datetime',
        '@{value}' : 'printf',
        '@{lower}' : 'printf',
        '@{upper}' : 'printf'
    }
)

df = pd.DataFrame(data=dict(date=dates, value=values, lower=lower, upper=upper))
source = ColumnDataSource(df)
p = figure(x_axis_type="datetime", y_range=(0, 9), plot_width=800, plot_height=350, tools=[hover1, WheelZoomTool(), PanTool(), ResetTool(),
p.xaxis.formatter=DatetimeTickFormatter(days=['%d %b'])
```

DataCite Commons

10.48366/r44930

Pages Support Sign In

Works People Organizations Repositories

Publication Year

- [ ] 2020 1

Work Type

- [ ] Dataset 1

License

- [ ] CC-BY-SA-4.0 1

1 Work

COVID-19 Reproductive Number Estimates

Allard Oelen, Jennifer D'Souza, Markus Stocker, Lars Vogt, Kheir Eddine Farfar, Muhammad Haris, Kamel Fadel, Mohamad Yaser Jaradeh & Vitalis Wiens

Comparison published 2020 in Open Research Knowledge Graph (ORKG)

Comparison of published reproductive number estimates for the COVID-19 infectious disease

DOI registered October 16, 2020 via DataCite.

Dataset English

https://doi.org/10.48366/r44930

DataCite Commons

10.48366/r44930

Works People

1 Work

COVID-19 Reproductive

Allard Oelen, Jennifer D'Souza, M

& Vitalis Wiens

Comparison published 2020 in Op

Comparison of published reprodu

DOI registered October 16, 2020 v

Dataset English

https://doi.org/10.48366/r449

Publication Year

2020 1

Work Type

Dataset 1

License

CC-BY-SA-4.0 1

19 References

Publication Year

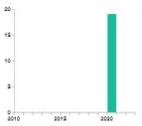

Pattern of early human-to-human tra

Julien Riou & Christian L. Althaus

Posted Content published 2020 in Crossref Citations

On December 31, 2019, the World Health Organizatio Wuhan, China. Chinese authorities later identified a n January 23, 2020, 655 cases have been confirmed in characteristics and the potential for sustained huma current screening and containment strategies, and d international concern (PHEIC). We performed stocha epidemiological findings to date. We found the basic indicating the potential for sustained human-to-hum magnitude to severe acute respiratory syndrome-re underline the importance of heightened screening, order to prevent further international spread of 2019

Other Identifiers

Publisher ID: biorxiv;2020.01.23.917351v1

DOI registered via Crossref.

2 Citations

Posted Content

https://doi.org/10.1101/2020.01.23.917351

Novel coronavirus 2019-nCoV: early predictions

Jonathan M Read, Jessica RE Bridgen, Derek AT Cum

Posted Content published 2020 in Crossref Citations

Since first identified, the epidemic scale of the recen rapidly, with cases arising across China and other co reproductive number of 3.11 (95%CI, 2.39-4.13); 58-7 ascertainment of 5.0% (3.6-7.4); 21022 (11090-33490

Other Identifiers

Publisher ID: medrxiv;2020.01.23.20018549v2

DOI registered via Crossref.

23 Citations

Posted Content

https://doi.org/10.1101/2020.01.23.20018549

Preliminary estimation of the basic r China, from 2019 to 2020: A data-driv

Shi Zhao, Qianyin Lin, Jinjun Ran, Salihu S Musa, Gui Maggie H Wang

Posted Content published 2020 in Crossref Citations

Other Identifiers

Publisher ID: biorxiv;2020.01.23.916395v2

DOI registered via Crossref.

7 Citations

Posted Content

https://doi.org/10.1101/2020.01.23.916395

Early Transmission Dynamics in Wuh

Qun Li, Xuhua Guan, Peng Wu, Xiaoye Wang, Lei Zhou Xing, Nijuan Xiang, Yang Wu, Chao Li, Qi Chen, Dan Li

Journal Article published 2020 in New England Jour

DOI registered February 16, 2020 via Crossref.

179 Citations

Journal Article

https://doi.org/10.1056/nejmoa2001316

Estimating the Unreported Number o First Half of January 2020: A Data-Driv

Zhao, Musa, Lin, Ran, Yang, Wang, Lou, Yang, Gao, He

Journal Article published 2020 in Journal of Clinical M

Background: In December 2019, an outbreak of respir China and has swiftly spread to other parts of China a reported roughly from 1 to 15 January 2020, and thus number, R0, of 2019-nCoV. Methods: We modelled the to 24 January 2020 through the exponential growth. T estimation. We used the serial intervals (SI) of infectio Respiratory Syndrome (SARS) and Middle East Respira nCoV to estimate R0. Results: We confirmed that the reporting was likely to have resulted in 469 (95% CI: 4 January 2020 was likely to have increased 21-fold (95 average. We estimated the R0 of 2019-nCoV at 2.56 (95 during the first half of January 2020 and should be co

DOI registered February 16, 2020 via Crossref.

11 Citations

Journal Article

https://doi.org/10.3390/jcm9020388

Nowcasting and forecasting the poter nCoV outbreak originating in Wuhan,

Joseph T Wu, Kathy Leung & Gabriel M Leung

Journal Article published 2020 in The Lancet

Other Identifiers

Publisher ID: S0140673620302609

DOI registered February 21, 2020 via Crossref.

86 Citations

Journal Article

https://doi.org/10.1016/s0140-6736(20)30260-9

Early Transmissibility Assessment of a

Maimuna Majumder & Kenneth D. Mandl

Journal Article published 2020 in SSRN Electronic Jou

DOI registered February 21, 2020 via Crossref.

5 Citations

Journal Article

https://doi.org/10.2139/ssrn.3524675

Estimation of the Transmission Risk o Interventions

Biao Tang, Xia Wang, Qian Li, Nicola Luigi Bragazzi, Sa

Journal Article published 2020 in SSRN Electronic Jou

DOI registered February 21, 2020 via Crossref.

4 Citations

Journal Article

https://doi.org/10.2139/ssrn.3525558

Real-Time Estimation of the Risk of De Inference Using Exported Cases

Sung-mok Jung, Andrei R. Akhmetzhanov, Katsuma H Kinoshita & Hiroshi Nishiura

Journal Article published 2020 in Journal of Clinical M

The exported cases of 2019 novel coronavirus (COVID- estimate the cumulative incidence and confirmed cas characterize the severity and understand the pandem exponential growth rate of the incidence, the present average number of secondary cases generated by a si from a single index case with illness onset on 8 Decem parameters (Scenario 2) based on data from 20 export January was estimated at 6924 cases (95% confidence respectively. The latest estimated values of the cCFR for Scenario 2. The basic reproduction number was es 2, respectively. Based on these results, we argued that pandemic. The proposed approach provides insights

DOI registered February 29, 2020 via Crossref.

7 Citations

Journal Article

https://doi.org/10.3390/jcm9020523

Estimation of the Transmission Risk of the 2019-nCoV and Its Implication for Public Health Interventions

Tang, Wang, Li, Bragazzi, Tang, Xiao & Wu

Journal Article published 2020 in Journal of Clinical Medicine

Since the emergence of the first cases in Wuhan, China, the novel coronavirus (2019-nCoV) infection has been quickly spreading out to other provinces and neighboring countries. Estimation of the basic reproduction number by means of mathematical modeling can be helpful for determining the potential and severity of an outbreak and providing critical information for identifying the type of disease interventions and intensity. A deterministic compartmental model was devised based on the clinical progression of the disease, epidemiological status of the individuals, and intervention measures. The estimations based on likelihood and model analysis show that the control reproduction number may be as high as 6.47 (95 interventions, such as intensive contact tracing followed by quarantine and iso number and transmission risk, with the effect of travel restriction adopted by t equivalent to increasing quarantine by a 100 thousand baseline value. It is essa measures implemented by the Chinese authorities can contribute to the preve long they should be maintained. Under the most restrictive measures, the outb January 2020) with a significant low peak value. With travel restriction (no imp infected individuals in seven days will decrease by 91.14% in Beijing, compare

DOI registered February 29, 2020 via Crossref.

10 Citations

Journal Article

https://doi.org/10.3390/jcm9020462

Report 3: Transmissibility of 2019-nCoV

N Imai, A Cori, I Dorigatti, M Baguelin, C Donnelly, S Riley & N Ferguson

Report published 2020 in Imperial College London

Self-sustaining human-to-human transmission of the novel coronavirus (2019-nCov) is the only plausible explanation of the scale of the outbreak in Wuhan. We estimate that, on average, each case infected 2.6 (uncertainty range: 1.5-3.5) other people up to 18th January 2020, based on an analysis combining our past estimates of the size of the outbreak in Wuhan with computational modelling of potential epidemic trajectories. This implies that control measures need to block well over 60% of transmission to be effective in controlling the outbreak. It is likely, based on the experience of SARS and MERS-CoV, that the number of secondary cases caused by a case of 2019-nCoV is highly variable – with many cases causing no secondary infections, and a few causing many. Whether transmission is continuing at the same rate currently depends on the effectiveness of current control measures implemented in China and the extent to which the populations of affected areas have adopted risk-reducing behaviours. In the absence of antiviral drugs or vaccines, control relies upon the prompt detection and isolation of symptomatic cases. It is unclear at the current time whether this outbreak can be contained within China; uncertainties include the severity spectrum of the disease caused by this virus and whether cases with relatively mild symptoms are able to transmit the virus efficiently. Identification and testing of potential cases need to be as extensive as is permitted by healthcare and diagnostic testing capacity – including the identification, testing and isolation of suspected cases with only mild to moderate disease (e.g. influenza-like illness), when logistically feasible.

Other Identifiers

Handle: 10044/1/77148

DOI registered March 6, 2020 via DataCite.

3 Citations

Text

https://doi.org/10.25561/77148

Time-varying transmission dynamics of Novel Coronavirus Pneumonia in China

Tao Liu, Jianxiong Hu, Jianpeng Xiao, Guanhao He, Min Kang, Zuhua Rong, Lifeng Lin, Haojie Zhong, Qiong Huang, Aiping Deng, Weilin Zeng, Xiaohua Tan, Siqing Zeng, Zhihua Zhu, Jiansen Li, Dexin Gong, Donghua Wan, Shaowei Chen, Lingchuan Guo & Yan Li

Posted Content published 2020 in Crossref Citations

Other Identifiers

Publisher ID: biorxiv;2020.01.25.919787v2

DOI registered March 12, 2020 via Crossref.

7 Citations

Posted Content

https://doi.org/10.1101/2020.01.25.919787

Modelling the epidemic trend of the 2019 novel coronavirus outbreak in China

Mingwang Shen, Zhihang Peng, Yanni Xiao & Lei Zhang

Posted Content published 2020 in Crossref Citations

We present a timely evaluation of the Chinese 2019-nCov epidemic in its initial phase, where 2019-nCov demonstrates comparable transmissibility but lower fatality rates than SARS and MERS. A quick diagnosis that leads to case isolation and integrated interventions will have a major impact on its future trend. Nevertheless, as China is facing its Spring Festival travel rush and the epidemic has spread beyond its borders, further investigation on its potential spatiotemporal transmission pattern and novel intervention strategies are warranted.

Other Identifiers

Publisher ID: biorxiv;2020.01.23.916726v1

DOI registered March 18, 2020 via Crossref.

5 Citations

Posted Content

https://doi.org/10.1101/2020.01.23.916726

Crossref

DataCite Commons

Type to search...

Pages Support Sign In

Works People Organizations Repositories

https://doi.org/10.1101/2020.03.08.20030643

Transmission potential of COVID-19 in Iran

Kamalich Muniz-Rodriguez, Isaac Chun-Hai Fung, Shayesterh R. Ferdosi, Sylvia K. Ofori, Yiseul Lee, Amna Tariq & Gerardo Chowell

Posted Content published 2020 via medRxiv

We computed reproduction number of COVID-19 epidemic in Iran using two different methods. We estimated R0 at 3.6 (95% CI, 3.2, 4.2) (generalized growth model) and at 3.58 (95% CI, 1.29, 8.46) (estimated epidemic doubling time of 1.20 (95% CI, 1.05, 1.44) days) respectively. Immediate social distancing measures are recommended.

Other Identifiers

Publisher ID: medrxiv;2020.03.08.20030643v1

DOI registered April 10, 2020 via Crossref.

2 Citations

Posted Content

https://doi.org/10.1101/2020.03.08.20030643

2 Citations

COVID-19 Reproductive Number Estimates

Allard Oelen, Jennifer D'Souza, Markus Stocker, Lars Vogt, Kheir Eddine Farfar, Muhammad Haris, Kamel Fadel, Mohamad Yaser Jaradeh & Vitalis Wiens

Comparison published 2020 in Open Research Knowledge Graph (ORKG)

Comparison of published reproductive number estimates for the COVID-19 infectious disease

DOI registered October 16, 2020 via DataCite.

Dataset English

https://doi.org/10.48366/r44930

Filter Works

Type to search...

Publication Year

2020 2

Work Type

Dataset 1

So why is most scientific information still buried in documents?

Because it is hard to produce FAIR scientific information

Post-publication / Manually

Basic reproduction number	3.1
location	Lombardy, Italy
Time period	2020-01-14 - 2020-03-08
research problem	Determination of the COVID-19

Cancel Create

Determination of the COVID-19 basic reproduction number
→ *Referred: 35 times* Instance of: *Problem*
ORKG

+ Add property

Post-publication / Automatically

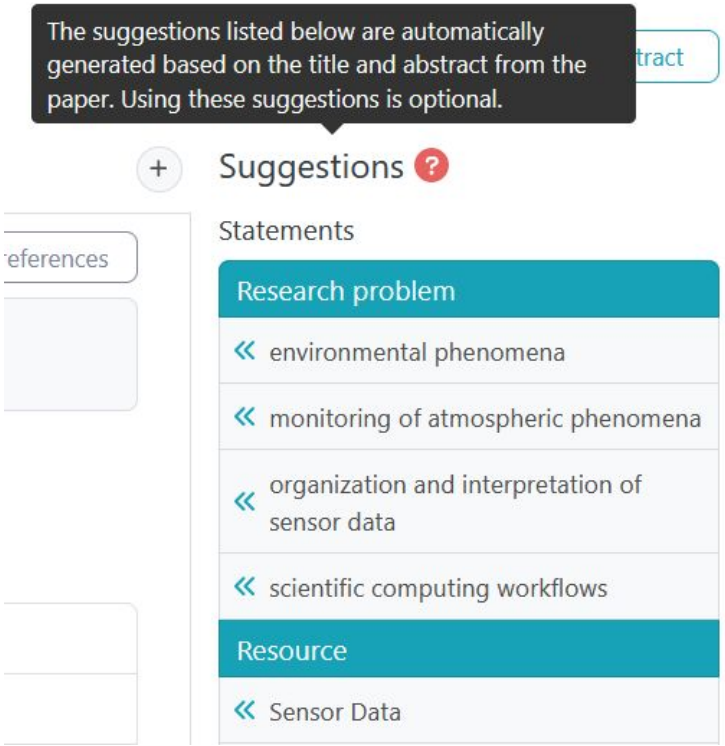

Pre-publication / FAIR at birth

Production

```r
# Two Linear Mixed Model (LMM) computations
lm.mwd.1 <- lmer(MWD_cor ~ cc_variant + (1|depth), data = df.MWD)
lm.mwd.2 <- lmer(MWD_cor ~ cc_type + (1|depth), data = df.MWD)

# Output data for the two LMM
df1 <- data.frame(summary(lm.mwd.1)$coefficients, check.names=FALSE)
df2 <- data.frame(summary(lm.mwd.2)$coefficients, check.names=FALSE)

instance <- tp$model_fitting(
  label="Linear mixed model fitting with MWD as response, CC variant as predictor variable, and soil depth as random variable",
  has_input_dataset=tuple(df.MWD, "Difference of mean weight diameter between the dry and wet sieving method"),
  has_input_model=tp$statistical_model(
    label="A linear mixed model with MWD as response and CC variant as predictor variable",
    is_denoted_by=tp$formula(
      label="The formula of the linear mixed model with MWD as response and CC variant as predictor variable",
      has_value_specification=tp$value_specification(
        label="MWD_cor ~ cc_variant + (1|depth)",
        has_specified_value="MWD_cor ~ cc_variant + (1|depth)"
      )
    )
  ),
  has_output_dataset=tuple(df1, "Results of LMM with MWD as response and CC variant as predictor variable")
)
instance$serialize_to_file("article.contribution.1.json", format="json-ld")
```

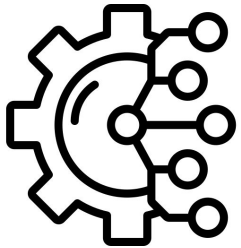

Pre-publication / FAIR at birth

Publication

Copernicus Publications

The Innovative Open Access Publisher

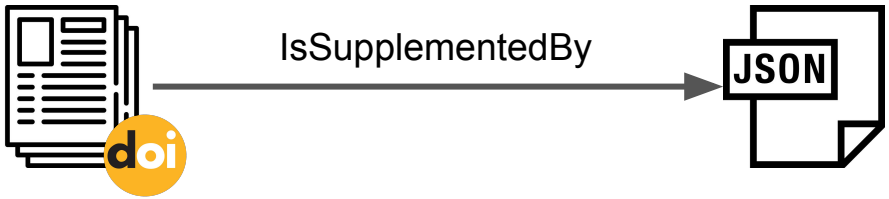

Pre-publication / FAIR at birth

Harvesting

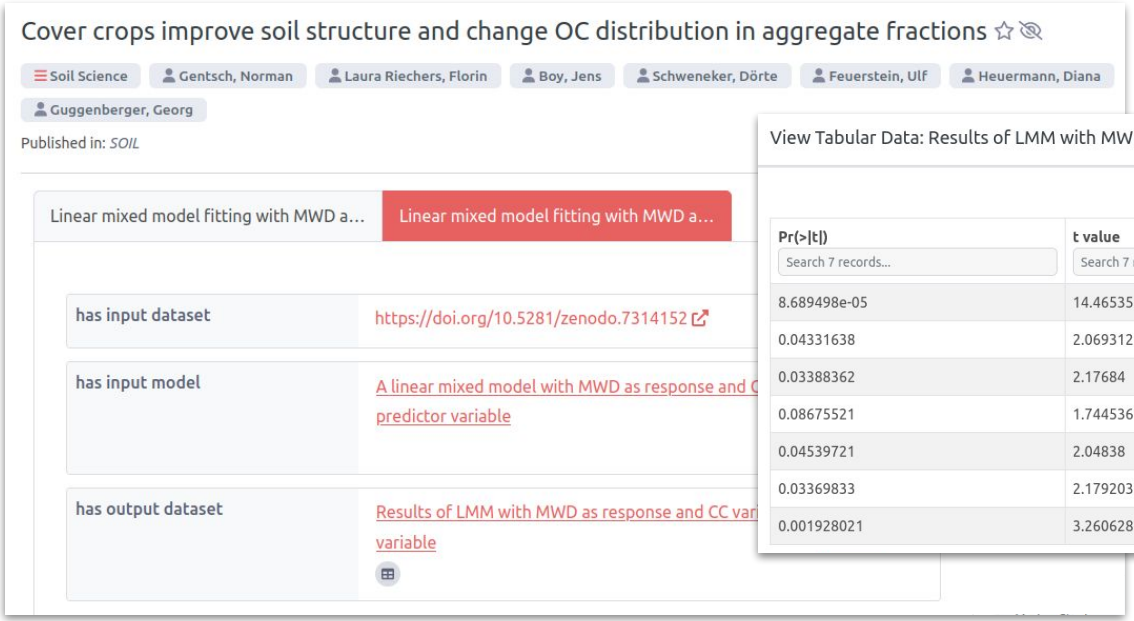

View Tabular Data: Results of LMM with MWD as response and CC variant as predictor variable

Pr(>|t|)	t value	df
Search 7 records...	Search 7 records...	Search 7 records...
8.689498e-05	14.46535	4.267258
0.04331638	2.069312	54.0
0.03388362	2.17684	54.0
0.08675521	1.744536	54.0
0.04539721	2.04838	54.0
0.03369833	2.179203	54.0
0.001928021	3.260628	54.0

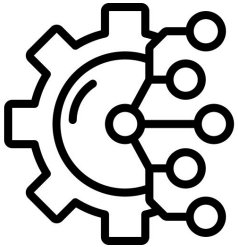

FAIR scientific information. It’s time.